Forest Systems
27(1), e004, 15 pages (2018)
eISSN: 2171-9845
https://doi.org/10.5424/fs/2018271-12658
Instituto Nacional de Investigación y Tecnología Agraria y Alimentaria O. A., M. P. (INIA)

RESEARCH ARTICLE

OPEN ACCESS

Applying quantitative structure models to plot-based terrestrial laser data to assess dendrometric parameters in dense mixed forests

Chiara Torresan[1], Ugo Chiavetta[1], and Jan Hackenberg[2]

[1]CREA- Research Centre for Forestry and Wood, Viale Santa Margherita 80, 52100 Arezzo, Italy. [2]Bigéochimie des Ecosystèmes Forestiers, INRA, Centre de Nancy, Route d'Amance, 54280 Champenoux, France.

Abstract

Aim of study: To assess terrestrial laser scanning (TLS) accuracy in estimating biometrical forest parameters at plot-based level in order to replace manual survey for forest inventory purposes.

Area of study: Monte Morello, Tuscany region, Italy.

Materials and methods: In 14 plots (10 m radius) in dense Mediterranean mixed conifer forests, diameter at breast height (DBH) and height were measured in Summer 2016. Tree volume was computed using the second Italian National Forest Inventory (INFC II) equations. TLS data were acquired in the same plots and quantitative structure models (QSMs) were applied to TLS data to compute dendrometric parameters. Tree parameters measured in field survey, *i.e.* DBH, height, and computed volume, were compared to those resulting from TLS data processing. The effect of distance from the plot boundary in the accuracy of DBH, height and volume estimation from TLS data was tested.

Main results: TLS-derived DBH showed a good correlation with the traditional forest inventory data (R^2=0.98, RRMSE=7.81%), while tree height was less correlated with the traditional forest inventory data (R^2=0.60, RRMSE=16.99%). Poor agreement was observed when comparing the volume from TLS data with volume estimated from the INFC II prediction equations.

Research highlights: The study demonstrated that the application of QSM to plot-based terrestrial laser data generates errors in plots with high density of coniferous trees. A buffer zone of 5 m would help reduce the error of 35% and 42% respectively in height estimation for all trees and in volume estimation for broadleaved trees.

Additional key words: LiDAR; geometrical modeling metrics; wood volume; forest inventory, tree segmentation; CompuTree; SimpleTree.

Abbreviations used: DBH (diameter at breast height); LiDAR (light detection and ranging); MAE (mean absolute error); MBE (mean bias error); MLESAC (maximum likelihood estimation sample consensus); MS (multiple scan); MSS (multiple-single scan); QSM (quantitative structure model); RMAE (relative value of mean absolute error); RMBE (relative value of mean bias error); RMSE (root-mean-squared error); RRMSE (relative value of root-mean-squared error); SS (single scan); TLS (terrestrial laser scanning).

Authors´ contributions: CT analyzed the data, did statistical analysis and interpretation of data, wrote the paper. UC conceived and designed the experiments, performed the experiments, coordinated the field activities, interpreted the data, revised the paper. JH provided support in the use of SimpleTree, revised the paper.

Citation: Torresan, C.; Chiavetta, U.; Hackenberg, J. (2018). Applying quantitative structure models to plot-based terrestrial laser data to assess dendrometric parameters in dense mixed forests. Forest Systems, Volume 27, Issue 1, e004. https://doi.org/10.5424/fs/2018271-12658

Received: 30 Nov 2017. **Accepted:** 25 Apr 2018.

Copyright © 2018 INIA. This is an open access article distributed under the terms of the Creative Commons Attribution 4.0 International (CC-by 4.0) License.

Funding: Field activities were funded by the LIFE CCM/IT/000905 LIFE FoResMit project.

Competing interests: The authors have declared that no competing interests exist.

Correspondence should be addressed to Chiara Torresan: chiara.torresan@crea.gov.it

Introduction

Terrestrial laser scanning (TLS), also known as ground-based Light Detection and Ranging (LiDAR), is an active remote sensing technique that acquires dense 3D point clouds from object surfaces using laser scanner. The introduction of TLS in the last two decades allowed for major changes in data collection for forest inventory purposes due to the possibility of rapid, automatic and periodic measurements of many important forest inventory attributes (Liang *et al.*, 2016). TLS allows measurements of 3D tree structure with millimeter-level detail and estimates of forest inventory attributes (Dassot *et al.*, 2012; Bauwens *et al.*, 2016).

The first studies which evaluated TLS for forest inventory, starting in the early 2000s, focused on tree attribute estimation (Simonse *et al.*, 2003; Aschoff

& Spiecker, 2004; Hopkinson *et al.*, 2004; Thies & Spiecker, 2004; Thies *et al.*, 2004; Watt & Donoghue, 2005; Henning & Radtke, 2006; Maas *et al.*, 2008). The main goal of these studies was to demonstrate the potential of TLS for faster and more accurate measurements compared to traditional field inventories. Later, the emphasis shifted to evaluating the capability of TLS to estimate stem and branch volume (Holopainen *et al.*, 2011; Dassot *et al.*, 2012), and biomass (Calders *et al.*, 2015; Ishak *et al.*, 2015; Rahman *et al.*, 2017) and important forest attributes not directly measured in conventional forest inventories, such as the volume of parts of trunk with certain radii and the branches of certain size (Raumonen *et al.*, 2013; Hackenberg *et al.*, 2015a). These later studies demonstrated that the precision of volume predictions from TLS were similar to those of predictions from allometric models.

For inventory purposes in circular sample plots, ground-based LiDAR data are acquired following three approaches (Liang *et al.*, 2016). In the first approach, single scan (SS), the laser scanner is located at the center of the plot and the trees are scanned by only one full field-of-view scan. In the second approach, multiple scan (MS), the laser scanner is placed in different locations inside and outside of the plot and a scan is carried out from each location. The point clouds generated from the scans are then co-registered by means of artificial reference targets. The third approach, multi-single scan (MSS), is similar to multiple scan, but without artificial reference targets. Instead, the co-registration is based on detected trees. Amongst the three approaches, the single scan approach is the simplest and fastest for data acquisition, but the occlusion of trees by other trees, branches and brush can result in the omission of up to 20% of the trees present in the plot (Mengesha *et al.*, 2015).

According to Bauwens *et al.* (2016), MS produces the best results to describe the upper part of the canopy with respect to the SS, while, according to Liang & Hyyppä (2013), the stem-detection accuracy is significantly improved using the MSS approach with respect to the single scan. A complication in the use of MSS is that matching the multiple data sets is difficult and can pose a problem. The MS approach seems to be the most accurate approach for mapping forest sample plots, allowing full coverage of the stem surface. It is also the method that requires the longest time to scan plots and post-process TLS data. While MS and MSS both represent improvements over single-scan, there is a lack of studies comparing the relative accuracy of the two approaches.

It is worth noting that studies have shown that for sites with rough terrain, the topographic relief causes more occlusion than tree stems (Trochta *et al.*, 2013). The standard method of selecting the position of a TLS instrument during a survey is currently made manually and subjectively by the operator on the basis of his or her skills and experience. Mozaffar & Varshosaz (2017) proposed a new automated algorithm that finds the optimum locations of a TLS, thus ensuring completeness of data and minimizing the number of scanning locations. The algorithm that they proposed is able to determine the station positions automatically and provided 99.5% coverage for simulated data and 91% coverage in real-world cases.

Regardless of the approach used to acquire TLS data, Newnham *et al.* (2015) assert that the use of terrestrial laser scanner for plot-scale measurements has not yet replaced manual measurement methods, in spite of the unparalleled structural information that it can capture, as it was anticipated more than 10 years ago from various authors. According to Newnham *et al.* (2015) "*the TLS has not come to fruition because the strength of TLS is not in replicating measurements that can be easily done manually*"; conversely it is "*in providing an assessment of structure that has not been achievable by any other means*". Newnham *et al.* (2015) are convinced that, to reach the full potential of this remote sensing instrument, it should not "*be viewed as a logical progression of existing plot-based measurement but it should be viewed as a disruptive technology that requires a rethink of vegetation surveys and their application across a wide range of disciplines*".

TLS data processing methods which allow the automatic reconstruction of accurate and precise 3D models of the tree were defined by Raumonen *et al.* (2013) as quantitative structure models (QSMs). QSMs allow one to derive geometrical modelling metrics in hard targets, such as tree stems and branches, which can be fully modelled (Newnham *et al.*, 2015). The models represent the trees as hierarchical collections of cylinders or other building blocks which provide the volume and diameter of branch segments needed to estimate the total above ground biomass. The theory behind some QSM deriving methods (Xu *et al.*, 2007; Livny *et al.*, 2010; Côté *et al.*, 2011, 2012) is based on the allometric scaling laws in biology (West *et al.*, 1997) which describes the distribution systems of vascular plants by branching network in which the sizes of tubes regularly decrease.

From allometric scaling laws, another basis for QSMs was derived: metabolic scaling theory (Enquist *et al.*, 2009) which provides "a quantitative, predictive framework for understanding the structure and dynamics of an average idealized forest" predicting a universal scaling law of tree growth by linking tree architecture to physiological function using fractals. These theories were tested by Bentley *et al.* (2013) who explored

patterns of external architecture within and across a tree by measuring the ratio radii/lengths and computing scaling exponents from five species. These concepts can be considered fundamental for the definition of QSM. In QSM, a tree is modeled as a hierarchical collection of cylinders (Raumonen *et al.*, 2013, 2015; Calders *et al.*, 2015) with additional assumptions about geometrical tree properties including branching structure, branching order, volumes, lengths, angles, and taper. Beside cylinders, in QSM other building blocks and "hybrid" models are used to model a tree such those reported in Åkerblom *et al.* (2015). The QSM approach has recently been expanded to 4D growth models by modifying theoretical plant growth algorithms to have stochastic components that produce the characteristics structural properties for each species (Potapov *et al.*, 2016). At the same time, theories of resource distribution networks, such as metabolic scaling theory, are being tested and further refined by the use of TLS data (Seidel, 2017; Trochta *et al.*, 2017). TLS can provide new approaches to the scaling of woody surface area and crown area, and thereby better quantify the metabolism of trees.

In addition to the QSM method, *i.e.* the cylinder approach, the voxel-based approach is used to develop solid models of trees (Gorte & Pfeifer, 2004; Moskal & Zheng, 2012; Vonderach *et al.*, 2012; Hosoi *et al.*, 2013; Bienert *et al.*, 2014). In this case, LiDAR-derived point-cloud data are converted for the target into voxels, and, from those volume elements, solid model of the entire tree − composed of consecutive voxels filling the outer surface and the interior of the stem, large and small branches − is obtained. In their study, Kunz *et al.* (2017) compared one voxel-based and two cylinder-based methods for wood volume estimation of 24 trees of *Acer platanoides* L., *Acer pseudoplatanus* L., *Sorbus aucuparia* L., and *Betula pendula* Roth, correlating the derived volume estimates from the point clouds with xylometric reference volumes for each tree. According to their results, the voxel-based method achieved the best results due to being more precise than cylinder-model based methods.

The objective of the present study was to assess TLS feasibility and accuracy in estimating biometrical forest parameters at plot-based level in dense Mediterranean mixed conifer plantations located in peri urban area using a QSM approach (Hackenberg, 2015a). In additional goal of the study was to confirm or to retract the conclusions of Newnham *et al.* (2015) about the inability of TLS to replace manual plot-based survey methods normally used in traditional forest inventory, to discuss if TLS could become an instrument operationally usable in forest inventories and under which conditions, and to eventually consider what operational measures can be adopted to increase estimation accuracy.

Material and methods

Study area and data collection

Study area

Monte Morello (934 m a.s.l.) is a mountain located NW of Florence (Tuscany region, Italy). According to Arrigoni *et al.* (1997), in the historic past browsing and grazing have considerably altered the forest vegetation of Monte Morello, while tillage has transformed it. At the beginning of 1800, the Monte Morello range substantially lacked vegetation. To reduce hydrogeological instability, which caused problems for the towns located on the slope of Monte Morello, in 1909, reforestation started and was conducted until the early years of the 1980's, with pauses during wartime (Maetzke, 2002). This reforestation allowed the restoration of the over-exploited woods higher up the slope (Arrigoni *et al.*, 1997). Conifer species, in particular black pine (*Pinus nigra* J. F. Arnold), Brutia pine (*Pinus brutia* Ten.), and Mediterranean cypress (*Cupressus sempervirens* L.), were chosen for their capability to colonize bare earth. They are responsible for the molding of the landscape around Florence which is characterized by pure or mixed high forests recognizable from far away in the city. For almost one century, few thinning interventions were done and this led to a scarce renovation of conifer species while the shade tolerant broadleaves species of the corresponding altitudinal layer returned to the understory, *i.e.* manna ash (*Fraxinus ornus* L.) as described by Gatteschi & Meli (1996).

The study area is located on the west side of Monte Morello. Stands are even-aged high forests composed of coniferous, mainly Brutia pine, black pine, Mediterranean cypress, and broadleaf, predominantly downy oak (*Quercus pubescens* Willd.) and Turkey oak (Quercus *cerris* L.) species. The presence of manna ash in the understory is also significant in terms of the number of trees, but less significant in terms of biomass. Table 1 describes the characteristics of forest site.

Dendrometric ground measurements

Dendrometric ground measurements were collected in 14 circular plots which were established for a previous study according to an unaligned systematic sampling design that allowed for ensuring of an adequate representation of all structural types in the forest stand of the study area (Fig. 1). The radius of each plot was 13 m, which corresponds to 530.93 m^2.

Field surveys were carried out during the summer (June-September) of 2016. The center of each circular

Table 1. Characteristics of Monte Morello study area

Location	Monte Morello
UTM 32N coordinates	679584.45 min East, 680022.46 max East, 4857883.75 min North, 4858759.15 max North
Surface	16.44 ha
Altitude (m a.s.l.)	min 554, max 637, mean 604
Slope (°)	min 2.05, max 20.15, mean 13.73
Mean annual temperature	13.9 °C
Annual rainfall	1003 mm
Soil type	Loam or clay loam texture, with average values of sand and clay of 38 and 28%, respectively. The soils were rich in carbonates and showed a moderately alkaline pH
Forest system	Planted forest
Tree species composition (% of total basal area)	43% Brutia pine, 31% European black pine 10% Turkey oak, 9% Italian cypress, 7% Other species
Forest age structure/Age in 2017	Two even-aged big groups 51 and 58 years

UTM=Universal Transverse Mercator

plot was identified with a chestnut stake emerging 40-50 cm above the ground level. For each tree with diameter at breast height (DBH) bigger or equal to 3.5 cm, the species, the healthy state (unharmed, broken or dead), and the DBH were recorded. The polar coordinates of each tree were collected using a TruPulse Laser Rangefinder 200/B (Laser Technology, Inc., Centennial, USA) and then converted into Cartesian coordinates with origin in the plot centre (Wilson 2000). For a subsample of 10 trees per plot, the height was also measured with a Haglof Vertex IV. These trees were selected subjectively in order to distribute height measures along the DBH range per each plot and to measure only trees with very visible tops.

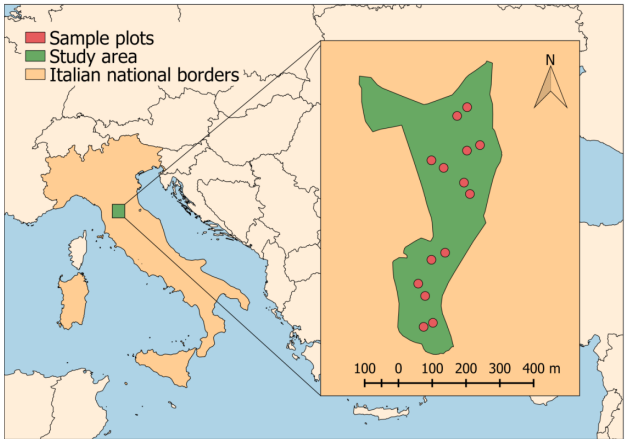

Figure 1. The location of the study area within the Italian national borders is represented by the green rectangle, and in detail the distribution of 14 plots within the study area.

Terrestrial Laser Scanner data collection

TLS data were acquired using a Focus3D X 130 (FARO Technologies Inc., Florida, USA). Features of the laser sensor are reported in Table 2. The laser scanner offers an integrated camera, allowing for post-scan acquisition of co-registered high-resolution RGB images.

Scanning activities were conducted from November 2015 to February 2016 (leaves off for broadleaves) in clear sky conditions and on windless days. For each plot, three scans were carried out by locating the

Table 2. Characteristics of Focus3D X 130 terrestrial laser scanner

Feature	Value
Weight	5.2 kg
Range determination	Phase-shift
Beam deflection principle	Rotating elliptical mirror
Laser wavelength	1550 nm
Range	0.6 – 130 m
Azimut range (horizontal field of view)	0° – 360°
Zenith range (vertical field of view)	0° – 300°
Nominally beam divergence	0.19 mrad
Number of returns/pulse	1
Measurements velocity	Up to 976000 points per second
Linearity error	± 2 mm
Integrated colored camera	70000000 pixel

scanner inside the borders of the plot at a distance of 3 to 6 m from the plot center and five to seven scans with the scanner external to the plot at a distance of 10-25 m from the plot centre. Twelve 14 mm diameter spheres were used for scan co-registration. This target type has been proven to be the most effective laser scanning target for co-registration because a spherical shape allows for the highest possible scanning efficiency from various directions and always provides a homogeneous reference surface (Brazeal, 2013). The targets were placed on poles at different heights and distributed throughout the plot both inside and outside (Fig. 2).

The laser scanner acquisition time for each scan was 7 min and 40 s with following parameters: scan angle, ±180°; resolution, 1/4; quality 3x; scan dimension, 10240 × 4267, 43.7 MPti; point distance, 6.136 mm/10 m.

Methods

Dendrometric data processing

From the ground data collected at plot level, the following variables have been computed for each plot: tree density, quadratic mean diameter, basal area, and mean height.

Volume for all live, unbroken trees was computed using the equations developed by Tabacchi *et al.* (2011) for the INFC II which allows the prediction of the aboveground tree volume using DBH and total tree height as independent variables for 25 of the most important forest species growing in Italy. In this study, tree volume is the volume of stem and branches with diameter equal to or bigger than 5 cm calculated with the INFC II species specific equations.

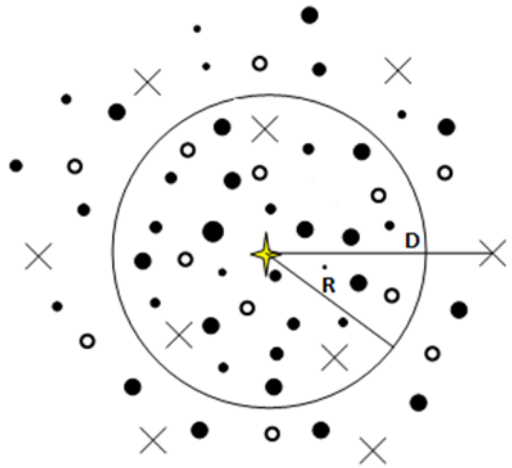

Figure 2. An example of scanning configuration for a plot. The sample plot is a circular area with radius R. The plot center is marked with a yellow star and the positions of the trees are shown as solid circles. Xs indicate the locations of the laser scanner instrument. The six scan positions external to the plot boundary are located in six quadrants with respect to the center of the plot (each quadrant resulting in 60°); the scans have a distance D from the center of the plot varying from 15 to 25 m. Spheres used for the co-registration of scans are shown as open circles.

TLS data processing

For each plot, scans were registered into a local coordinate system by the reference sphere using Trimble RealWorks Software (Trimble Inc., Sunnyvale, CA, USA).

Successive TLS data processing was performed using the open source platform Computree (Othmani *et al.*, 2011) which integrates various plugins each composed of various steps; for this reason in the following description the name of the plugin and step, as called in Computree platform, are provided in italic within bracket.

First of all, each registered point cloud was pre-elaborated to trade-off completeness of field information and elaboration time needed. For these purposes, each point cloud obtained from the registration process was translated to have its coordinate system origin at the plot center coherent with the field survey (*toolkit plugin, TK_TranslateCloud step*). Then, the point cloud was clipped with a 10 m radius cylinder centered at the plot center (*onf plugin, ONF_StepExtractPlot step*).

Successively, QSMs of trees were built to produce cylinders which describe the complete above-ground woody tree components in a topologically order (Åkerblom *et al.*, 2017). The reproducible pipe line consisted in these main phases:

(i) Classification of returns into ground and non-ground points and DTM generation: returns were classified as ground points (*onf plugin, ONF_StepClassifyGround step*), noise was removed from detected points (*simpletree plugin, ST_StepFilterGroundPoints step*) and the DTM was created (*onf plugin, ONF_stepComputeDTM02 step*).

(ii) Generation of seed points: to produce the seeds needed in the tree segmentation process, from the non-ground points, a slice parallel to the DTM at a height between 1.30 m and 1.60 m was extracted (*simpletree plugin, ST_StepExtractSliceAboveDTM step*). The slice was successively denoised to eliminate the type vegetation, such as shrubs, felled trees, etc., that can compromise the detection of tree stems (*simpletree plugin, ST_StepFilterStems, ST_StepExtractLargestCluster, ST_StepExtractSliceAboveDTM, ST_StepMergeClouds, ST_StepClearSky, ST_StepExtractSliceAboveDTM steps*). To the obtained denoised slice, Euclidean clustering operation (*simpletree plugin, ST_StepEuclideanClustering step*) was applied pro-ducing two output clouds, one

containing all large clusters and one all small clusters, allowing the former ones the identification of points belonging to the stems, *i.e.* the seed points, from which to start segmenting a tree.

(iii) Tree segmentation: starting from seeds obtained at the phase (ii), individual tree segmentation was performed (*simpleree plugin, ST_StepSegmentationAll step*).

(iv) Fitting tree models by cylinders using QSMs and applying allometric correction: preliminary steps were the application of denoising filters to the clusters (*onf plugin, ONF_StepFilterClustersBySize step; simpletree plugin, ST_StepFilterClusters, ST_StepStatisticalOutlierRemoval, ST_StepSplitByHeight, ST_StepExtractLargestCluster, ST_StepMergeClouds, ST_StepVoxelGridFilter steps*) which allowed us obtain clear trees to enhance the results of the application of the QSM sphere following method to fit tree branches by cylinders with allometric correction (*simpletree plugin, ST_StepCompleteFolderModelling2 step*).

(v) Computing dendrometric parameters: coordinates of tree position, DBH, height, and volume were computed and saved in a result list file, while data describing each cylinder obtained from the QSM sphere following method, *e.g.* branch order, start (x,y,z), end (x,y,z), radius, length, etc., were saved in a user-specific folder in a second file per tree (*simpletree plugin, ST_StepExportAll step*).

The version of SimpleTree plugin used in this study was the 4.30.1 (Hackenberg *et al.*, 2015a).

Despite the pipeline being equally performed for all plots, the parameterization was plot-specific, this means that for each plot specific values of parameters in each single step were set. This was necessary to adapt the process to the peculiarity of each plot in term of site morphology, and forest structure (*i.e.* tree and underwood density, young trees, uprooted trees, etc.).

Specifically concerning the algorithms applied in the QSM approach of SimpleTree plugin, details will be available in the deliverable "Algorithms for automatic tree detection, stem form in 3D and cloud density for small branches from TLS" of the EU project Diabolo or from the free available source code. Henceforth we will only give a summary. The QSM method utilized in SimpleTree is based on the usage of search spheres which reconstruct the structure from the roots to the tree tips following the tree branches (Hackenberg *et al.*, 2014, 2015b). For each search sphere, if its center is approximately located on the tree skeleton and its radius is larger than the according tree components radius will have on its surface points representing cross sectional areas. A circle is fitted with the Maximum Likelihood Estimation Sample Consensus (MLESAC) algorithm (Torr & Zisserman, 2000), its radius is stored, then enlarged by a factor of ~2 and finally converted to a new 3D sphere so the procedure can be repeated recursively. In case of branch junctions, multiple circles can be fitted. Two successively fitted circles are combined to build a cylinder. The procedure terminates when the sphere reaches the tip of the tree or a large gap between the points which can occur in case of occlusion. In these cases, the attractor technique developed by Côté *et al.* (2011; 2012) is utilized by the SimpleTree plugin to allow the method to estimate also cylinders geometry in large occluded areas. After the cylinders derived from circle fits are generated, they are improved by the plugin through the MLESAC algorithm for cylinder fitting. This algorithm allows robust fitting of models due to its high tolerance of outliers in the experimental data that has been applied to a wide range of model parameter estimation problems in computer vision, *e.g.* feature matching, registration or detection of geometric primitives (Fischler & Bolles, 1981). The SimpleTree approach also includes an allometric scaling theory based improvement which takes into consideration the relationship between the growth volume of a generated cylinder, that is the volume of the generated cylinder plus the growth volume of all the cylinder's children, and its radius. The function allows for the identification of cylinders with an overestimated volume which are outliers of the function, so in this way the radius of cylinder is adjusted to be in accordance with its fixed growth volume (Hackenberg *et al.*, 2015a).

Statistical analysis

Tree detection analysis was conducted by computing the relative value of detection rate, comparing the number of trees surveyed in each plot with the number of trees segmented by QSM method in the same plot. In addition, the value of the detection rate was calculated by considering the entire number of surveyed trees within 5 cm-wide DBH classes.

Differences between positions of trees recorded during the field campaign and the position resulting from the QSM process were computed only for trees recognized to be homologous. Influence of DBH and distance from plot border in the accuracy of tree position were explored.

Tree parameters measured in field survey, *i.e.* DBH, height, and volume computed from the INFC II equations, were compared to those resulting from TLS data processing.

Considering that a combination of metrics are often required to assess model performance (Chai & Draxler, 2014), the determination coefficient (R^2), root-mean-squared error (RMSE), relative value of the RMSE (RRMSE), mean absolute error (MAE), relative value of the MAE (RMAE), mean bias error (MBE) and relative mean bias error (RMBE) were calculated to compare

predictions and observations. MAE was calculated because according to Wilmott & Matsuura (2005) this dimensioned statistics is a more natural measure of average error. MBE was reported with the intention to indicate average model "bias", that is average over- or underprediction (Wilmott & Mat-suura, 2005).

RMSE, for n different predictions corresponding to the number of trees, was computed as following:

$$RMSE = \sqrt{\frac{\sum_{i=1}^{n}(\widehat{y_i}-y_i)^2}{n}} \quad [1]$$

where $\hat{y}_i$ is the predicted value for i-th tree and y_i is the observed value for the same i-th tree.

RRMSE was computed as the RMSE in percent over the mean observed value of the target variable, to able to compare the results obtained in this study with those obtained in other researches.

MAE was computed as following:

$$MAE = \frac{\sum_{i=1}^{n}|\widehat{y_i}-y_i|}{n} \quad [2]$$

and the RMAE was computed as the MAE in percent over the mean observed value of the target variable.

The MBE was computed as the difference between the model-predicted and observed means respectively, as following:

$$MBE = \frac{\sum_{i=1}^{n}(\widehat{y_i}-y_i)}{n} \quad [3]$$

and the RMBE was computed as the MBE in percent over the mean observed value of the target variable.

The edge effect, *i.e.* the effect of distance from the plot boundary, in the accuracy of DBH, height and volume estimation from TLS data was tested to evaluate the influence of buffer size from the plot border in the performance of biometric variable estimation.

Statistical analysis was performed with R (R Core Team, 2013).

Results

Plot level dendrometric data processing results

Table 3 reports the values of basal area for each tree species in the plot and the corresponding values in terms of percent composition for all 14 plots.

In Table 4, average values for the dendrometric parameters of all trees with DBH equal or bigger than 3.5 cm of 14 plots are reported. Density ranges between 923 and 2420 trees per hectare, while quadratic mean diameter ranges between 15 and 36 cm, and the height of trees surveyed between 12 and 22 m. Data analysis allowed for the identification of 6 groups of plots according to their structural characteristics. A group (Plot_1_1, 1_2, 2_1 and 2_2) includes pure and almost pure plots of Brutia pine (from 100% to 89.7%) with quadratic mean diameter from 32 cm to 36 cm, a second group includes plots within adult stands mixed of Brutia pine, other coniferous, pubescent oak and other broadleaves (Plot_3_1 and 3_2), a third group

Table 3. Values of basal area for the species in each plots with the values of tree species composition in percent within the square bracket. Pb=*Pinus brutia* Ten., Pn=*Pinus nigra* J.F. Arnold, Cs=*Cupressus sempervirens* L., Oc=other coniferous, Fo=*Fraxinus ornus* L., Qc=*Quercus cerris* L., Qp=*Quercus pubescens* Willd., Ob=other broadleaves

Plot	Basal area (m²/ha)							
	Pb	Pn	Cs	Oc	Fo	Qc	Qp	Ob
1_1	83.19 [100.0]	-	-	-	-	-	-	-
1_2	92.70 [89.7]	-	2.31 [6.9]	-	0.12 [3.4]	-	-	-
2_1	99.50 [90.0]	-	1.10 [2.5]	-	0.51 [5.0]	-	-	0.14 [2.5]
2_2	90.56 [95.6]	-	-	-	0.38 [4.4]	-	-	-
3_1	55.74 [37.8]	3.46 [2.2]	-	-	1.23 [17.8]	1.14 [2.2]	11.43 [24.4]	1.46 [15.6]
3_2	38.03 [46.7]	-	-	0.88 [10.0]	0.40 [10.0]	-	12.16 [30.0]	0.17 [3.3]
5_1	-	51.90 [35.9]	-	-	2.19 [45.3]	11.47 [15.6]	-	0.16 [3.1]
5_2	-	60.11 [32.9]	5.23 [5.3]	-	3.58 [46.1]	1.38 [2.6]	-	1.06 [13.2]
6_1	-	12.88 [7.9]	2.15 [2.6]	-	5.28 [60.5]	21.36 [18.4]	-	1.06 [10.5]
6_2	-	39.55 [31.8]	11.22 [16.7]	-	3.59 [45.5]	-	-	0.65 [6.1]
7_1	-	44.12 [27.5]	4.29 [5.8]	5.17 [1.4]	3.73 [56.5]	4.59 [8.7]	-	-
7_2	-	38.20 [37.5]	14.36 [27.1]	-	0.84 [20.8]	11.86 [12.5]	-	0.29 [2.1]
9_1	-	45.02 [20.0]	13.68 [22.7]	0.51 [1.3]	3.38 [53.3]	-	-	0.14 [2.7]
9_2	-	31.19 [31.0]	23.33 [35.7]	-	0.69 [28.6]	0.36 [4.8]	-	-

Table 4. Mean values of dendrometric parameters of each of 14 plots of 10 m of radius

Plot	Mean tree age (years)	Density (trees/ha)	Quadratic mean diameter (cm)	Basal area (m^2/ha)	Mean measured height (m)
1_1	51	1018.59	32.25	83.19	20.94
1_2	51	923.10	36.22	95.13	23.32
2_1	51	1273.24	31.83	101.25	20.05
2_2	51	1432.39	28.43	90.94	20.56
3_1	51	1432.39	25.73	74.46	18.89
3_2	51	954.93	26.24	51.64	18.18
5_1	58	2037.18	20.27	65.72	17.79
5_2	58	2419.16	19.38	71.38	17.09
6_1	58	2419.16	15.00	42.73	14.06
6_2	58	2100.85	18.26	55.01	12.93
7_1	58	2196.34	18.95	61.90	13.73
7_2	58	1527.89	23.37	65.55	15.32
9_1	58	2387.32	18.29	62.73	16.22
9_2	58	1336.90	23.01	55.57	18.23

is represented by plots within young stands mainly composed of European black pine and manna ash with a tree density ranging from 2000 to 2400 trees/ha (Plot_5_1, 5_2 and 6_2). Another group includes plots within stands composed of European black pine, Tuscan cypress, and manna ash with a tree density ranging from 1300 to 1500 trees/ha (Plot_9_2 and 7_2). Another group of plots was found within stands mainly composed of manna ash, European black pine and Tuscany cypress with a tree density around 2300 trees/ha (Plot_7_1 and 9_1), and a plot almost completely composed of small broadleaves trees (manna ash and pubescent oak) with high tree density (Plot_6_1).

Tree detection results

The results of tree detection from the individual tree segmentation process are reported in Table 5 which compares the number of trees surveyed in each plot with the number of segmented trees and shows the percentage of trees not detected (*i.e.* false negative) and the percentage of clusters erroneously detected as trees (*i.e.* false positive). In general the rate of false positive is higher than the rate of false negative, which is due to the fact that the QSM process reconstructed scattered groups of returns as trees. Plots with the most false positives are those which contain a high number of young manna ash stems, which occurs in the lower canopy layer (see characteristics of plots in Table 3).

Fig. 3 shows the number and percentage of detected, not detected and over detected trees in relation to the DBH. The highest detection rate is for the trees with a stem diameter between 25 cm and 35 cm. In the case of a stem with a diameter between 10 cm and 20 cm there is an over-detection, this means that the segmentation process generates more trees than are actually present in the plots.

The matching process between the coordinates of trees recorded during inventory campaign and those obtained from the tree segmentation allowed 491 tree pairs to be found. The accuracy of the tree position obtained as output of the QSM with respect to field position is reported in Table 6 as minimum, maximum, mean and standard deviation, and distance from plot centre RMSE and its relative pendant RRMSE.

In Fig. 4, positioning deviation in relation to field inventory DBH (a) and the tree distance from plot center (b) are represented. Neither the DBH nor the distance from the center to the boundary of the plot seem to influence the position deviation.

Tree DHB, height and volume prediction

Reference data DBH values regressed against TLS DBH values are plotted in Fig. 5: the linear regression shows a determination coefficient of 0.98, a RMSE equal to 1.75 cm, and a RRMSE equal to 7.81% (Fig. 5a). MAE and RMAE are respectively equal to 0.89 cm and 3.99%, while MBE and RMBE are respectively -0.81 cm and -3.64%. The residual plot (Fig. 5b) shows a fairly random pattern, indicating a good fit for a linear model and the absence of any influence of DBH on the estimation error.

Table 5. Results from the process of tree segmentation

Plot	Number of trees (DBH ≥3.5 cm)	Number of segmented trees (DBH ≥3.5 cm)	% of trees not detected (false negative)	% of trees over detected (false positive)
1_1	32	32	0	0
1_2	29	33	0	13.8
2_1	40	41	0	2.5
2_2	45	43	4.4	0
3_1	45	55	0	22.2
3_2	30	37	0	23.3
5_1	64	54	15.6	0
5_2	76	68	10.5	0
6_1	76	73	3.9	0
6_2	66	80	0	21.2
7_1	69	75	0	8.7
7_2	48	53	0	10.4
9_1	75	95	0	26.7
9_2	42	45	0	7.1

DBH=diameter at breast height

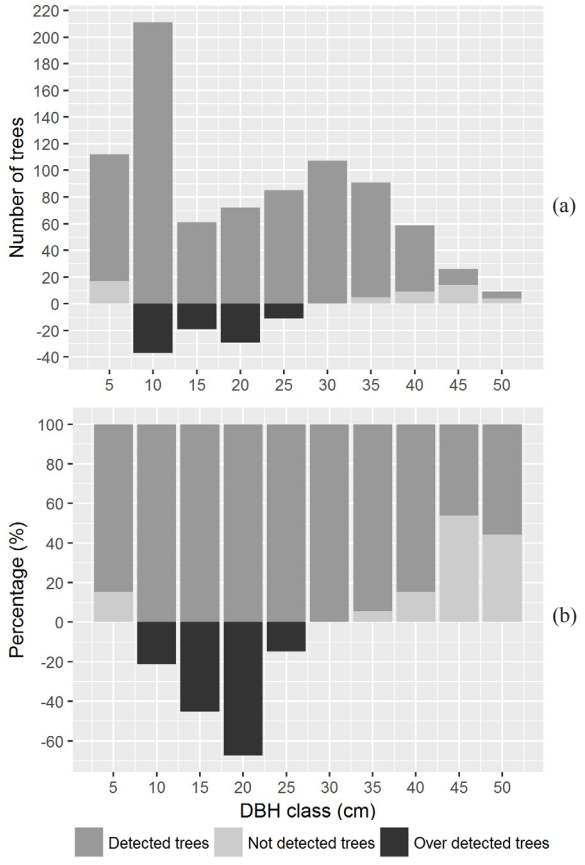

Figure 3. Number (a) and percentage (b) of detected, not detected and over detected trees per diameter class. Diameter at breast height (DBH) values referred to the upper boundary of the DBH interval, *e.g.,* 10 cm is the range 5 cm ≤ DHB < 10 cm

Table 6. Accuracy of tree position in 491 trees

Min deviation	0.019 m
Max deviation	1.496 m
Mean deviation	0.489 m
Standard deviation	0.309 m
Distance from plot centre RMSE	0.348 m
Distance from plot centre RRMSE	5.63%

RMSE=root-mean-squared error. RRMSE=relative value of RMSE

The reference data height regressed against TLS height is plotted in Fig. 6a: the R^2 is 0.60, the RMSE is 3.00 m, the RRMSE is 16.99%, the MAE is 1.02 m and the RMAE is 5.80%. The MBE and RMBE are respectively -0.81 m and -4.59%. Tree heights tended to be underestimated by TLS for trees up to approximately 10 m tall and overestimated for trees above this height (Fig. 6b).

Concerning the volume estimation for all species of trees, *i.e.* coniferous and broadleaved, volume computed with the INFC II equations regressed against tree volume inferred using QSMs applied to the TLS data shows moderate low degree of correlation and an overestimation was observed. When only broadleaved trees are considered, the performance increases (R^2=0.64, RMSE=0.27 m^3, RRMSE=137.08%, MAE= 0.16 m^3, and RMAE=82.25%, MBE=0.16 m^3, RMBE= 82.25%), as seen in Fig. 7.

The effect of distance from plot boundary in RMSE and R^2 of DBH, height and volume estimation are

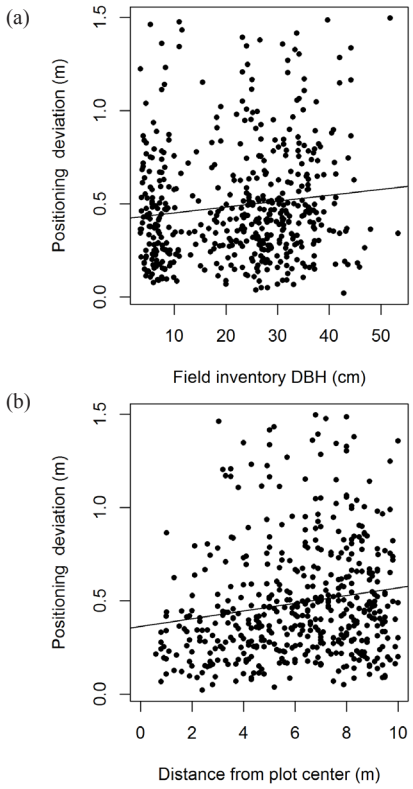

Figure 4. Positioning deviation in relation to field inventory diameter at breast height (DBH) (a) and the distance from plot center (b)

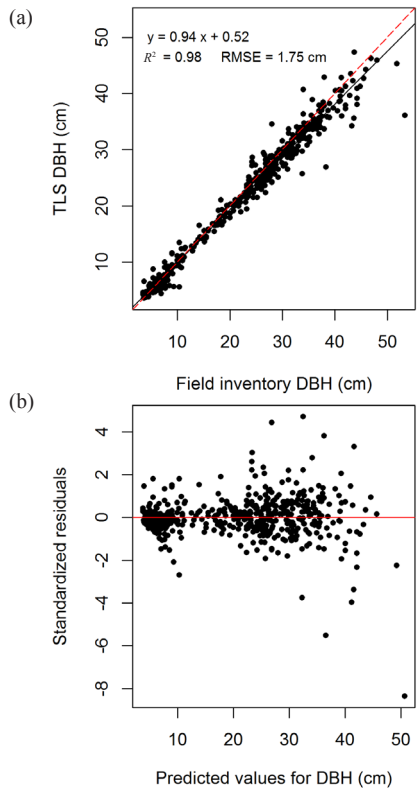

Figure 5. Field inventory diameter at breast height (DBH) against terrestrial laser scanner (TLS) DBH (a) and standardized residuals distribution (b)

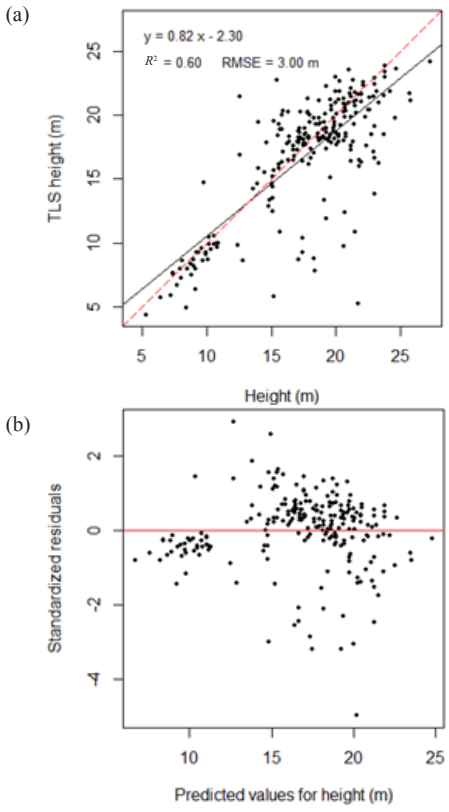

Figure 6. Field inventory height against terrestrial laser scanner (TLS) height (a) and standardized residuals distribution (b)

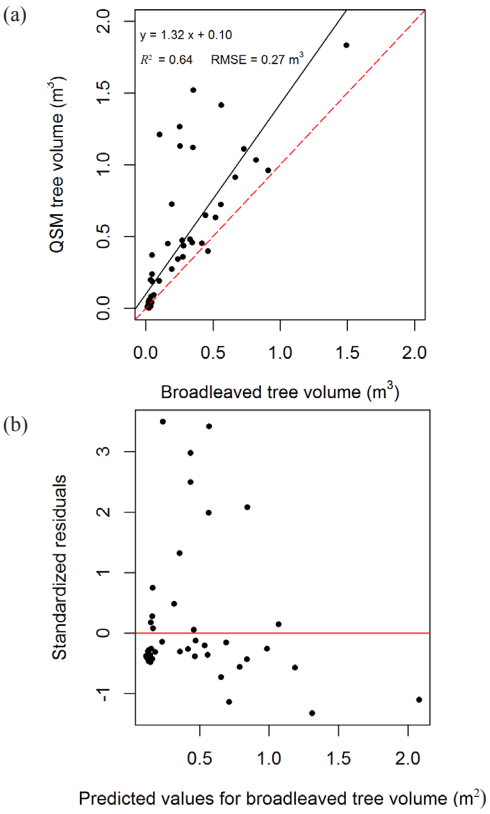

Figure 7. Italian National Forest Inventory (INFC) volume of broadleaved tree against quantitative structure model (QSM) volume and standardized residuals distribution

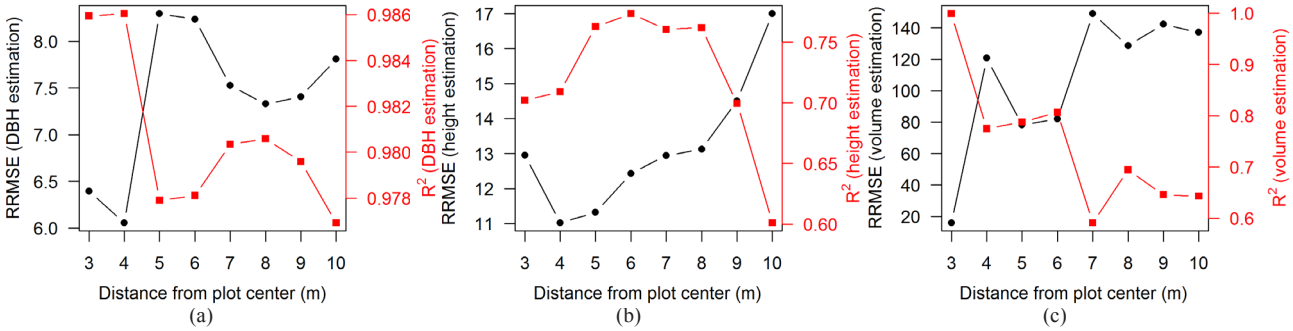

Figure 8. Diameter at breast height (DBH) (a), height (b), and volume (c) estimation accuracy (RRMSE and R^2) with different values of distance from plot center

reported in Figs. 8. With reference to DBH estimation from TLS data, Fig. 8a shows that the highest estimation accuracy is achieved at a distance of 4 m from the plot center; when moving toward the border of the plot the accuracy decreases. A buffer of about 6 m from the boundary of the plot seems to be a safe approach to increase the estimation of this variable. A sharp increase in tree height estimation accuracy with TLS data occurs when trees are located farther from the border of the plot (Fig. 8b), this means that the accuracy of tree height estimation from TLS data is strongly influenced by the distance from plot border. A smaller estimation error resulted for trees located within 5 m from the plot center. The threshold of distance from the plot center that marks a big difference in volume estimation accuracy for broadleaved trees is 5 m (Fig. 8c): volume estimation accuracy decreases in a wide band approximately 5 m from plot border.

Discussion

The first consideration is about structural and specific heterogeneity of plots. A sample of plots differentiated in terms of structural and specific characteristics provides a good chance to represent local considerations and determine whether the rate of detection is eventually influenced by those aspects.

The application of QSM in TLS data allowed for the extraction of single trees and the assessment of tree variables at plot level in mixed forests.

Tree segmentation and fitting cylinders detected a larger number of trees, which resulted in an overall false negative rate of 9%. It is worth mentioning that the QSM method requires many parameters to be set, in all phases except for the QSM step in which a fully automatic parameters search was used. For this reason, the detection error seems to be related to the peculiarity of the forest structure of each plot rather than to the QSM method. In some plots, the stems lying on the ground, fallen or uprooted as a consequence of scarce thinning intervention in the forest, generated objects which have been segmented as trees. The results from the detection process of this study confirmed what Liang *et al.* (2016) found in many investigations carried out from 2004 to 2014: the detection rate decreases as the stem density increases. In fact, in our study, the highest levels of overestimation were reached in plots with a density bigger than 2100 trees/ha, while in plots with stem density up to 1200 trees/ha the detection rate was around 100%. In this study, the number of non-detected trees was highest for trees with a DBH above 35 cm. Comparing this result with that of other studies is difficult, because this result is affected by the scheme used in the scan data acquisition and by the season of surveys, *i.e.* leaf-on or leaf-off period. We observed that the number of trees inventoried for diameter class 40 cm, 45 cm and 50 cm respectively were 60, 27 and 11. The number of trees not segmented in the same class were 9, 14, and 5 respectively (15%, 52% and 45%), see Fig. 3b. If we consider the amount of trees inventoried, the trees not segmented in these diameter classes correspond to 3.8% of all trees in field. Considering that their incidence is small with respect the total amount of trees, we are not able to statistically identify the factors that influenced this aspect.

Stem position was determined with a standard deviation of 0.56 m, but the range between the minimum (0.02 m) and maximum deviation (1.50 m) was quite large. Tests made in the field to evaluate the reliability of the instruments that measure the parameters needed for tree position determination in the field, angle and distance of tree from the station, demonstrated that these values are not stable and could be affected by magnetic fields. Anyway, it is difficult to say if the reference value of position should come from traditional instruments or from a terrestrial laser scanner. The comparison of DBH values obtained from the application of QSM in TLS data with those measured in field showed a satisfying level of accuracy (R^2=0.98, RMSE=1.75 cm, and RRMSE=7.81%). This result is congruent with the study of Calders *et al.* (2015)

carried out in a plot of 40 m radius where five scans were executed: the RMSE in Calders *et al.* (2015) was 2.39 cm in a sample of 75 trees. It seems important to point out that similar results were obtained in studies that use the single-scan approach. For example, Maas *et al.* (2008) in a plot of 15 m radius with a density of 212-240 stems/ha obtained a RMSE ranging between 1.8-3.3 cm, Brolly & Kiraly (2009) in a plot of 30 m radius with a density of 753 stems/ha obtained a RMSE ranging between 3.4 cm and 7.0 cm. But also Liang & Hyyppa (2013) in plot of 10 m radius with a density ranged between 605 and 1210 stems/ha obtained a RMSE between 0.7 and 2.4 cm, and Olofsson *et al.* (2014) in plot of 20 m of radius with 358-1042 stems/ha reached a RMSE between 2.0 and 4.2 cm. DBH is the biometrical parameter estimated with the highest performance from TLS data.

On the contrary, the comparison of field inventory tree heights against TLS-derived tree heights from the application of QSMs did not show a good linear fit (R^2=0.60). Unfortunately, also the studies cited above − Maas *et al.* (2008), Liang & Hyyppa (2013), Olofsson *et al.* (2014) − did not obtain reassuring results reporting RMSE respectively of 4.6 m, 2.0-6.5 m, 4.9 m, which are greater than the RMSE reported in this study (3.00 m). At the moment, these results do not come out in favor of TLS data for very accurate height estimation, regardless of the method used to extract single trees and to compute the height, and regardless of the mode used for scanning the plots (single or multi-scan modes). These low values of accuracy are most probably due to the uncertainty of the visibility of treetops in TLS data which lead to underestimated heights and to a magnitude of the estimation error typically around meters. This is particularly severe in coniferous species due to needle occlusion in TLS surveys. Tree height measurements using TLS for forest inventories need to be thoroughly studied because the height values invalidate consequent volume estimation values. At the same time, it is important emphasize that better results have been obtained in case of height measured with traditional instruments (*e.g*. measuring tape or Laser Tech Impulse) in harvested trees: this means that we have to take in consideration that subjectivity at height measurement came with the large applicability of modern instruments, such as Vertex. According to Vasilescu (2013), the user error caused by the sight line at the top of tree is 0.3 m for the smaller tree (about 10 m height) and less than 0.2 m in case of taller trees (height bigger than 20 m). Larjavaara & Muller-Landau (2013) confirmed that laser rangefinder tree height measurements which used the sine method resulted in systematic underestimation by 20% on average with respect to instruments using the tangent method. On the other hand, TLS surveys carried out during leaf-off season in case of broadleaved forests, can increase the accuracy of height estimation using TLS data (Srinivasan *et al.*, 2015).

The performance of the volume estimates using the QSMs, evaluated by comparing this volume to the volume predicted using the Italian nationwide volume models developed by Tabacchi *et al.* (2011), was weak in case of all species, with a general trend of overestimation by the QSMs. According to Calders *et al.* (2015), possible error sources that can cause overestimation can be related to TLS data, including registration error, occlusion, wind and noise, or to QSM reconstruction, such as segmentation and geometric structure error due to cylinder versus real branch or leaf shape. In fact, according to Kunz *et al.* (2017), high values of accuracy in tree volume calculation from point clouds applying cylinder model approaches scanning were reached using TLS data of single trees that were scanned from different position, for example from four positions perpendicular to each other. In this case, volume was estimated with a determination coefficient of 0.89 and 0.92 using the Raumonen *et al.* (2013) and the Hackenberg *et al.* (2014) approaches respectively. The results from their studies confirmed that excellent results can be obtained when QSMs are applied at the level of single tree instead of plot level and targeting merchantable volumes instead of total volume. In this study, data were acquired at plot level and cloud segmentation was performed at the plot level; moreover, total volume was considered instead of merchantable volume as the most common target variable in forest inventories. Furthermore, occlusions in the top of tree crown can be important, which sometimes leads to the reconstruction of branches that are not actually present, and consequently the volume of those branches is estimated. It is known that the stem is the tree component that contributes most to the total volume of a tree, but when tree density is high the occlusions are also high, so the estimation errors will increase. In fact, the performance of QSM increases in case of broadleaved trees: this leads to considering needle noise as a key source of error. Stovall *et al.* (2017) have highlighted that this approach can result in unexpected and unrealistic volumes in dense or clumped tree canopies that have significant occlusion such as those caused by needles. In particular, results in the supplementary material of Stovall *et al.* (2017) show high good fitting quality on an isolated stems above ground biomass (R^2=0.98), while model performance decreases when branches with needles, which increases noise, are included (R^2=0.42).

It is also worth underlining that the allometric models used for volume estimation are valid for the all national territories, and using an allometric models in areas with different climatic, geographic, and silvicultural

conditions to those where the models were developed may lead to large errors in the estimates (Liang *et al.*, 2014, 2016).

This study allowed us to understand that the position of trees with respect to the plot boundary influenced the quality of estimation of the biometrical parameters. This is probably due to the condition of trees at the edge of the clipped point cloud. In fact, to clipping the point cloud abruptly is a mandatory step in the TLS plot data preparation. As a consequence many trees effectively present in the plot can be partially erased from the cloud compromising the next steps. From this result, an important outcome follows: when TLS data are processed, a buffer zone should be considered around the area under investigation as proposed by Calders *et al.* (2015) and the data analysis should be undertaken in this extended area, and at the end of data analysis, the trees that are located in the buffer zone should be excluded. In this way, it is possible to take advantage of the positive effect of a buffer area to improve the estimates. This threshold can be 4-5 m for stands structurally similar to the sample plots used in this study. This finding can be relevant to significantly increasing the accuracy of tree height and broadleaved tree volume estimates (35% and 42% increase of RRMSE respectively) to acceptable values at plot level. This outcome can help in planning the TLS surveys and the computational procedures.

The QSM approach allows for the extraction of a large number of parameters, for instance branch order, angle and radius, ovality of the stem, open stem height etc. This can be very useful for analysis in commercial forests with less complex structure compared with our dense sample stands with dense understorey vegetation. Definitively, terrestrial LiDAR is a remote sensing technology that should be exploited beyond forest inventory purposes. Stronger effort should be put to the analysis of the information obtained from the products derived from TLS for to use them for ecological purposes (*e.g.* growth monitoring, disturbance assessing, structural indices extraction etc.).

References

Åkerblom M, Raumonen P, Kaasalainen M, Casella E, 2015. Analysis of geometric primitives in quantitative structure models of tree stems. Remote Sens 7: 4581-4603. https://doi.org/10.3390/rs70404581

Åkerblom M, Raumonen P, Mäkipää R, Kaasalainen M, 2017. Automatic tree species recognition with quantitative structure models. Remote Sens Environ 191: 1-12. https://doi.org/10.1016/j.rse.2016.12.002

Arrigoni PV, Foggi B, Bechi N, Ricceri C, 1997. Documenti per la carta della vegetazione del Monte Morello (Provincia di Firenze). Parlatorea II: 73-100.

Aschoff T, Spiecker H, 2004. Algorithms for the automatic detection of trees in laser scanner data. ISPRS 36: 66-70.

Bauwens S, Bartholomeus H, Calders, Lejeune P, 2016. Forest inventory with terrestrial LiDAR: A comparison of static and hand-held mobile laser scanning. Forests 7 (6): 127-143. https://doi.org/10.3390/f7060127

Bentley LP, Stegen JC, Savage VM, Smith DD, von Allmen EI, Sperry S, Reich PB, Enquist BJ, 2013. An empirical assessment of tree branching networks and implications for plant allometric scaling models. Ecol Lett 16 (8): 1069-1078. https://doi.org/10.1111/ele.12127

Bienert A, Hess C, Maas HG, Von Oheimb G, 2014. A Voxel-based technique to estimate the volume of trees from terrestrial laser scanner data. International archives of the photogrammetry, remote sensing and spatial information sciences - ISPRS Archives 40 (5): 101-106.

Brazeal R, 2013. Low cost spherical registration targets for terrestrial laser scanning. SUR 6905 - Point Cloud Analysis.

Brolly G, Kiraly G, 2009. Algorithms for stem mapping by means of terrestrial laser scanning. Acta Silvatica et Lignaria Hung 5: 119-130.

Calders K, Newnham G, Burt A, Murphy S, Raumonen P, Herold M, Culvenor D, Avitabile L, Disney M, Armston J, Kaasalainen M, 2015. Nondestructive estimates of above-ground biomass using terrestrial laser scanning. Meth Ecol Evol 89: 86-93. https://doi.org/10.1111/2041-210X.12301

Chai T, Draxler RR, 2014. Root mean square error (RMSE) or mean absolute error (MAE)? - Arguments against avoiding RMSE in the literature. Geosci Model Dev 7: 1247-1250. https://doi.org/10.5194/gmd-7-1247-2014

Côté JF, Fournier RA, Egli R, 2011. An architectural model of trees to estimate forest structural attributes using terrestrial LiDAR. Environ Model Softw 26: 761-777. https://doi.org/10.1016/j.envsoft.2010.12.008

Côté JF, Fournier RA, Frazer GW, Niemann KO, 2012. A fine-scale architectural model of trees to enhance LiDAR-derived measurements of forest canopy structure. Agr Forest Meteorol 166: 72-85. https://doi.org/10.1016/j.agrformet.2012.06.007

Dassot M, Colin A, Santenoise P, Fournier M, Constant T, 2012. Terrestrial laser scanning for measuring the solid wood volume, including branches, of adult standing trees in the forest environment. Comp Electron Agr 89: 86-93. https://doi.org/10.1016/j.compag.2012.08.005

Enquist BJ, West GB, Brown JH, 2009. Extensions and evaluations of a general quantitative theory of forest structure and dynamics. P Nat Acad Sci USA 106 (17): 7046-7051. https://doi.org/10.1073/pnas.0812303106

Fischler MA, Bolles RC, 1981. Random sample consensus: A paradigm for model fitting with application to image analysis and automated cartography. Commun ACM 24 (6): 381-395. https://doi.org/10.1145/358669.358692

Gatteschi P, Meli R, 1996. I rimboschimenti di Monte Morello 85 anni dopo (1909-1994) [Monte Morello reforestation 85 years later (1909-1994)]. L'Italia Forestale e Montana 4: 231-249.

Gorte B, Pfeifer N, 2004. Structuring laser scanned trees using 3D mathematical morphology. Int Archiv Photogramm Remote Sens 35 (B5): 929-933.

Hackenberg J, Morhart C, Sheppard J, Spiecker H, Disney M, 2014. Highly accurate tree models derived from terrestrial laser scan data: a method description. Forests 5: 1069-1105. https://doi.org/10.3390/f5051069

Hackenberg J, Spiecker H, Calders K, Disney M, Raumonen P, 2015a. SimpleTree —An efficient open source tool to build tree models from TLS clouds. Forests 6: 4245-4294. https://doi.org/10.3390/f6114245

Hackenberg J, Wassenberg M, Spiecker H, Sun D, 2015b. Non destructive method for biomass prediction combining TLS derived tree volume and wood density. Forests 6 (4): 1274-1300. https://doi.org/10.3390/f6041274

Henning JG, Radtke PJ, 2006. Detailed stem measurements of standing trees from ground-based scanning Lidar. Forest Sci 52 (1): 67-80.

Holopainen M, Vastaranta M, Kankare V, Räty M, Vaaja M ,Liang X, Yu X, Hyyppä J, Hyyppä H, Viitala R, Kaasalainen S, 2011. Biomass estimation of individual trees using stem and crown diameter TLS measurements. Int Archiv Photogramm Remote Sens Spat Inf Sci - ISPRS Archiv 38 (5W12): 91-95.

Hopkinson C, Chasmer L, Young-Pow C, Treitz P, 2004. Assessing forest metrics with a ground-based scanning lidar. Can J Forest Res 34 (3): 573-583. https://doi.org/10.1139/x03-225

Hosoi F, Nakai Y, Omasa K, 2013. 3-D voxel-based solid modeling of a broad-leaved tree for accurate volume estimation using portable scanning lidar. ISPRS J Photogramm Remote Sens 82: 41-48. https://doi.org/10.1016/j.isprsjprs.2013.04.011

Ishak NI, Abu Bakar MA, Abdul Rahman MZA, Rasib AW, Kanniah KD, Meng Shin AL, Razak KA, 2015. Estimating single tree stem and branch biomass using terrestrial laser scanning. Jurnal Teknologi 77 (26): 59-67. https://doi.org/10.11113/jt.v77.6860

Kunz M, Hess C, Raumonen P, Bienert A, Hackenberg J, Maas HG, Härdtle W, Fichtner A, Von Oheimb G, 2017. Comparison of wood volume estimates of young trees from terrestrial laser scan data. iForest 10: 451-458.

Larjavaara M, Muller-Landau HC, 2013. Measuring tree height: a quantitative comparison of two common field methods in a moist tropical forest. Meth Ecol Evol 4 (9): 793-801. https://doi.org/10.1111/2041-210X.12071

Liang X, Hyyppä J, 2013. Automatic stem mapping by merging several terrestrial laser scans at the feature and decision levels. Sensors 13: 1614-1634. https://doi.org/10.3390/s130201614

Liang X, Kankare V, Yu X, Hyyppa J, Holopainen M, 2014. Automated stem curve measurement using terrestrial laser scanning. IEEE Trans Geosci Remote Sens 52: 1739-1748. https://doi.org/10.1109/TGRS.2013.2253783

Liang X, Kankare V, Hyyppä J, Wang Y, Kukko A, Haggrén H, Yu X, Kaartinen H, Jaakkola A, Guan F, *et al.*, 2016. Terrestrial laser scanning in forest inventories. ISPRS J Photogramm Remote Sens 115: 63-77. https://doi.org/10.1016/j.isprsjprs.2016.01.006

Livny Y, Yan F, Olson M, Chen B, Zhang H, El-Sana J, 2010. Automatic reconstruction of tree skeletal structures from point clouds. ACM Trans on Graphics 29 (6): 151. https://doi.org/10.1145/1882261.1866177

Maas HG, Bienert A, Scheller S, Keane E, 2008. Automatic forest inventory parameter determination from terrestrial laser scanner data. Int J Remote Sens 9 (5): 1579-1593. https://doi.org/10.1080/01431160701736406

Maetzke F, 2002. I rimboschimenti di Monte Morello: analisi e indirizzi di un progetto aperto per la loro rinaturalizzazione [The reforestations of Monte Morello: analysis and addresses of an open project for their renaturalisation] L'Italia Forestale e Montana 2: 125-138.

Mengesha T, Hawkins M, Nieuwenhuis M, 2015. Validation of terrestrial laser scanning data using conventional forest inventory methods. Eur J Forest Res 134: 211-222. https://doi.org/10.1007/s10342-014-0844-0

Moskal LM, Zheng G, 2012. Retrieving forest inventory variables with terrestrial laser scanning (TLS) in urban heterogeneous forest. Remote Sens 4: 1-20. https://doi.org/10.3390/rs4010001

Mozaffar MH, Varshosaz M, 2017. Optimal placement of a terrestrial laser scanner with an emphasis on reducing occlusions. The Photogrammetric Record 31 (156): 374-393. https://doi.org/10.1111/phor.12162

Newnham GJ, Armston JD, Calders K, Disney MI, Lovell JL, Schaaf CB, Strahler AH, Danson FM, 2015. Terrestrial laser scanning for plot-scale forest measurements. Curr Forest Rep 1: 239-251. https://doi.org/10.1007/s40725-015-0025-5

Olofsson K, Holmgren J, Olsson H, 2014. Tree stem and height measurements using terrestrial laser scanning and the RANSAC algorithm. Remote Sens 6: 4323-4344. https://doi.org/10.3390/rs6054323

Othmani A, Piboule A, Krebs M, Stolz C, Lew Yan Voon LFC, 2011. Towards automated and operational forest inventories with T-Lidar. 11th Int Conf on LiDAR Applications for Assessing Forest Ecosystems (SilviLaser 2011), Oct 2011, Hobart, Australia.

Potapov I, Järvenpää M, Åkerblom M, Raumonen P, Kaasalainen M, 2016. Data-based stochastic modeling of tree growth and structure formation. Silva Fennica 50 (1): 1-11. https://doi.org/10.14214/sf.1413

R Core Team, 2013. R: A language and environment for statistical computing. R Foundation for Statistical Computing, Vienna, Austria. http://wwwR-projectorg/.

Rahman MZA, Bakar MAA, Razak KA, Rasib AW, Kanniah KD, Kadir WHW, Omar H, Faidi A, Kassim AR, Latif ZA, 2017. Non-destructive, laser-based individual tree aboveground biomass estimation in a tropical rainforest. Forests 8 (86): 1-22. https://doi.org/10.3390/f8030086

Raumonen P, Kaasalainen M, Akerblom M, Kaasalainen S, Kaartinen H, Vastaranta M, Holopainen M, Disney M, Lewis P, 2013. Fast automatic precision tree models from terrestrial laser scanner data. Remote Sens 5 (2): 491-520. https://doi.org/10.3390/rs5020491

Raumonen P, Casella E, Calders K, Murphy S, Åkerblom M, Kaasalainen M, 2015. Massive-scale tree modelling from TLS Data. ISPRS Annals of the Photogrammetry, Remote Sensing and Spatial Information Sciences, Volume II-3/W4, 2015, PIA15+HRIGI15 - Joint ISPRS Conf 2015, 25-27 March, Munich. https://doi.org/10.5194/isprsannals-II-3-W4-189-2015

Seidel D, 2017. A holistic approach to determine tree structural complexity based on laser scanning data and fractal analysis. Ecol Evol 8 (1): 128-134. https://doi.org/10.1002/ece3.3661

Simonse M, Aschoff T, Spiecker H, 2003. Automatic determination of forest inventory parameters using terrestrial laser scanning. Proc Scan Laser Scientific Workshop on Airborne Laser Scanning of Forests, Umea, Sweden. pp: 251-257.

Srinivasan S, Popescu SC, Eriksson M, Sheridan RD, Ku NW, 2015. Terrestrial laser scanning as an effective tool to retrieve tree level height, crown width, and stem diameter. Remote Sens 7: 1877-1896. https://doi.org/10.3390/rs70201877

Stovall AEL, Vorster AG, Anderson RA, Evangelista PH, Shugart HH, 2017. Non-destructive aboveground biomass estimation of coniferous trees using terrestrial LiDAR. Remote Sens Environ 200: 31-42. https://doi.org/10.1016/j.rse.2017.08.013

Tabacchi G, Di Cosmo L, Patrizia G, 2011. Aboveground tree volume and phytomass prediction equations for forest species in Italy. Eur J Forest Res 130 (6): 911-934. https://doi.org/10.1007/s10342-011-0481-9

Thies M, Spiecker H, 2004. Evaluation and future prospects of terrestrial laser scanning for standardized forest inventories. Int Archiv Photogramm Remote Sens Spat Inf Sci XXXVI - 8/W2. http://citeseerx.ist.psu.edu/viewdoc/summary?doi=10.1.1.221.8063

Thies M, Pfeifer N, Winterhalder D, Gorte BGH, 2004. Three-dimensional reconstruction of stems for assessment of taper, sweep and lean based on laser scanning of standing trees. Scand J Forest Res 19 (6): 571-581. https://doi.org/10.1080/02827580410019562

Torr PHS, Zisserman A, 2000. MLESAC: A new robust estimator with application to estimating image geometry. Comp Vision Image Underst 78 (1): 138-156. https://doi.org/10.1006/cviu.1999.0832

Trochta J, Král K, Janík D, Adam D, 2013. Arrangement of terrestrial laser scanner positions for area-wide stem mapping of natural forests. Can J For Res 43: 355-363. https://doi.org/10.1139/cjfr-2012-0347

Trochta J, Krůček M, Vrška T, Král K, 2017. 3D Forest: An application for descriptions of three-dimensional forest structures using terrestrial LiDAR. PLoS ONE 12 (5): e0176871 https://doi.org/10.1371/journal.pone.0176871

Vasilescu MM, 2013. Standard error of tree height using Vertex III. Bull Transilvania Univ of Braşov Series II: Forest Wood Indus Agr Food Eng 6 (55-2): 2013.

Vonderach C, Voegtle T, Adler, P, 2012. Voxel-based approach for estimating urban tree volume from terrestrial laser scanning data. Int Arch Photogramm Remote Sens Spatial Inf Sci XXXIX-B8: 451-456. https://doi.org/10.5194/isprsarchives-XXXIX-B8-451-2012

Watt PJ, Donoghue DNM, 2005. Measuring forest structure with terrestrial laser scanning. Int J Remote Sens 26 (7): 1437-1446. https://doi.org/10.1080/01431160512331337961

West GB, Brown JH, Enquist BJ, 1997. A general model for the origin of allometric scaling laws in biology. Science 276 (5309): 122-126. https://doi.org/10.1126/science.276.5309.122

Willmott CJ, Matsuura K, 2005. Advantages of the mean absolute error (MAE) over the root mean square error (RMSE) in assessing average model performance. Clim Res 30: 79-82. https://doi.org/10.3354/cr030079

Wilson AD, 2000. New methods, algorithms, and software for rapid mapping of tree positions in coordinate forest plots. Res Pap SRS-19. Asheville, NC: USDA For Serv, South Res Stat. 31 p. https://www.srs.fs.usda.gov/pubs/rp/uncaptured/rp_srs019.pdf

Xu H, Gosset N, Chen B, 2007. Knowledge and heuristic-based modeling of laser scanned trees. ACM Trans Graphics 26(4): 19. https://doi.org/10.1145/1289603.1289610